We are IntechOpen, the world's leading publisher of Open Access books Built by scientists, for scientists

6,900
Open access books available

186,000
International authors and editors

200M
Downloads

154
Countries delivered to

Our authors are among the

TOP 1%
most cited scientists

12.2%
Contributors from top 500 universities

CLARIVATE ANALYTICS
BOOK CITATION INDEX
INDEXED

WEB OF SCIENCE™

Selection of our books indexed in the Book Citation Index
in Web of Science™ Core Collection (BKCI)

Interested in publishing with us?
Contact book.department@intechopen.com

Influence of Current Pulse Shape on Directly Modulated Systems Using Positive and Negative Dispersion Fibers

Paloma R. Horche[1] and Carmina del Río Campos[2]
[1]ETSI Telecomunicación, Universidad Politécnica de Madrid,
[2]Escuela Politécnica Superior, Universidad San Pablo CEU,
Spain

1. Introduction

The proliferation of high-bandwidth applications has given rise to a growing interest, between network providers, on upgrading networks to deliver broadband services to homes and small businesses. There has to be a good balance between the total cost of the infrastructures and the services that can be offered to the end users, as they are very sensitive to equipment outlay, requiring the use of low-cost optical components. Coarse Wavelength Division Multiplexing (CWDM) is an ideal solution to the tradeoff between cost and capacity (Thiele, 2007). This technology uses all or part of the 1270 to 1610 nm wavelength fiber range with an optical channel separation of about 20 nm. This channel separation allows the use of low-cost, uncooled, Directly Modulated Lasers (DML). The main advantages of these devices associated with uncooled operation are (Nebeling, 2007); No integration of TEC and cooler required, less complexity for control electronics, reduced power consumption, only laser diode current required, lower device cost. Otherwise, the direct modulation of the laser current leads to a modulation of the carrier density giving rise to a *chirp frequency*. This results in a broadened linewidth and a laser wavelength drift (Henry, 1982; Linke, 1985). Since wavelength chirp was recognized several years ago, (Koch, 1988; Hinton, 1993) many papers have addressed the causes and implications of chirp on the optical system performance (Cartledge, 1989; Hakki, 1992; Horche, 2008). However, a large part of the research has focused on fiber transmission properties. The idea of these studies is, generally, based on considerations regarding the interaction of the laser frequency chirp with the fiber dispersion. It is known that if the chirp parameter (α-factor) is positive, as is always the case for directly modulated lasers, then the frequency components of the leading edge of the pulse will be blue-shifted and the trailing edge red-shifted. If the pulses are transmitted over a negative dispersion fiber where the blue wavelength is slower than the red, to some extent, pulse compression and significant transmission performance improvement is expected (Morgado & Cartaxo, 2001; Tomkos et al., 2001).

To counteract the effect of chromatic dispersion, the system can be moved to a non-zero negative dispersion-shifted fiber, but this method has some problems that are difficult to resolve when it comes to a CWDM metropolitan or access network; The traffic must be interrupted. This method may only be used for upgrading long wavelength channels where

this fiber has much lower dispersion values. And, cost-effectiveness, changing the fiber is expensive both to buy and to lay.

In DMLs, the frequency chirp for large-signal modulation can be determined from the shape of the electric pulse applied to the optical source (modulation current) (Coldren & Corzini, 1995). Since the DML chirp parameter is tunable through the modulation current applied to the diode laser, optimum operating-conditions in terms of the chirp/dispersion interactions can be set for fibers having different amounts and signs of dispersion.

It is the aim of this Chapter to discuss and compare how the shape of the modulated signal (e.g, exponential-wave, sine-wave, Gaussian, etc.) can improve the system performance when using both positive and negative dispersion fibers. With this method it is possible to improve each of the WDM system channels individually, offering a low-cost solution since it only involves changes in the transmitters and avoiding the replacement of the fiber.

The aim of this chapter is also to present analytical and simulation results pertaining to the transmission of chirped optical signals in a dispersive fiber.

This Chapter is organized as follows: Section 2 deals with the theoretical background of optical fiber dispersion; In Section 3 we analyze the power and chirp waveforms for different DMLs both theoretically and by simulation; Sections 4 and 5 focus on the study of the interplay between the laser chirp and the dispersion of both Gaussian pulses and pulses of an arbitrary shape, upon which the subject of this work is based; Section 6 details the system modeling together with the presentation of the parameters used in our simulation for the different fibers, DMLs and modulation current; Section 7 discusses the simulation results for the determination of the optimum modulation current under different scenarios; Section 8 studies the accumulated phase along the link as a method of improving the system performance. In Section 9 we analysis the transmission performance over different lengths of positive and negative dispersion fibers through computer simulation. Finally, a brief summary and the conclusions are presented in Section 10.

2. Factors contributing to dispersion in optical fibers

When a short pulse of light travels through an optical fiber, its power is "dispersed" in time so that the pulse spreads into a wider time interval. The principal sources of dispersion in single optical fibers are material dispersion, waveguide dispersion, polarization-mode dispersion and non-linear dispersion. The combined contributions of these effects to the spread of pulses in time are not necessarily additive (Agrawal, 2010).

The PMD-induced pulse broadening is characterized by the root mean-square (RMS) $\sigma_T \equiv D_p\sqrt{L}$, where D_p is the PMD parameter. Measured values of D_p vary from fiber to fiber in the range D_p = 0.01–1 ps/$\sqrt{km}$. Because of the $\sqrt{L}$ dependence, PMD induced pulse broadening is relatively small compared with the other effects. Indeed, for fiber lengths < 400 km, as is the case of metro-CWDM systems, the PMD can be ignored.

The combined effects of material dispersion and waveguide dispersion which is referred to as chromatic dispersion is, in general, the major source of pulse broadening and it may be determined by including the wavelength dependence of the optical fiber refractive indices, n_1 and n_2 when determining $d\beta/d\omega$ from the characteristic equation of the fiber.

Since β is a slowly varying function of this angular frequency, one can see where various dispersion effects arise by expanding β in a Taylor series about a central frequency ω_0 (Keiser, 2010). Expanding β in a Taylor series yields

$$\beta(\omega)=\beta_0+\beta_1(\omega-\omega_0)+\frac{1}{2}\beta_2(\omega-\omega_0)^2+\frac{1}{6}\beta_3(\omega-\omega_0)^3+\cdots \tag{1}$$

where β_m denotes the mth derivative of β with respect to ω evaluated at $\omega = \omega_0$.

From (1) it can be obtained the velocity at which the energy in a pulse travels along a fiber (*group velocity*) and the *group-velocity dispersion* parameter, known as the GVD, which determines how much an optical pulse would broaden on propagation inside the fiber. They are defined as

$$v_g = \frac{1}{\left.\dfrac{\partial\beta(\omega)}{\partial\omega}\right|_{\omega=\omega_0}} = \frac{1}{\beta_1} \quad ; \quad GVD = \left.\frac{\partial^2\beta(\omega)}{\partial\omega^2}\right|_{\omega=\omega_0} \equiv \beta_2 \tag{2}$$

In some optical communications systems, the frequency spread $\Delta\omega$ is determined by the range of wavelengths $\Delta\lambda$ emitted by the optical source. It is customary to use $\Delta\lambda$ in place of $\Delta\omega$. By using $\omega = 2\pi c/\lambda$, 24) can be written as

$$D = -\frac{2\pi c}{\lambda^2}\beta_2 \tag{3}$$

where D is called the *dispersion parameter* and is expressed in units of ps/(km·nm).

In the fourth term of (1), the factor of β_3 is known as the *third-order dispersion*. This term is important around the wavelength at which β_2 is equal to zero (*zero-dispersion wavelength*). Higher-order dispersive effects are governed by the dispersion slope $S = dD/d\lambda$. The parameter S is also called a *differential-dispersion* parameter. By using (3), it can be written as

$$\beta_3 = \frac{\partial\beta_2}{\partial\omega} = -\frac{\lambda^2}{2\pi c}\frac{\partial\beta_2}{\partial\lambda} = -\frac{\lambda^2}{2\pi c}\frac{\partial}{\partial\lambda}\left[-\frac{\lambda^2}{2\pi c}D\right] \tag{4}$$

$$S = \frac{4\pi c}{\lambda^3}\beta_2 + (\frac{2\pi c}{\lambda^2})^2\beta_3 \quad \left[\frac{ps}{(nm)^2\cdot km}\right] \tag{5}$$

The numerical value of the dispersion slope S plays an important role in the design of CWDM systems. Since $S > 0$ for most fibers, different channels have slightly different GVD values. This feature makes it difficult to compensate dispersion for all channels simultaneously.

3. Directly modulated laser

DFB lasers are the workhorse in WDM systems, both as cooled and uncooled devices. In order to provide cost-effective solutions for CWDM systems, directly modulated, uncooled distributed feedback (DFB) lasers are preferred (DFB-DML).

As regards cost, CWDM systems are usually single-span (unlike their DWDM counterparts), inasmuch as they do not use any type of in-line optical amplification. Since there is no optical amplification, the output power of the laser needs to be sufficient to sustain the system's loss budget. This involves the transmission fiber, multiplexer loss together with additional splice and connector losses.

A typical N-wavelength CWDM system, as standardized in ITU-T G.695, is shown in Fig. 1.
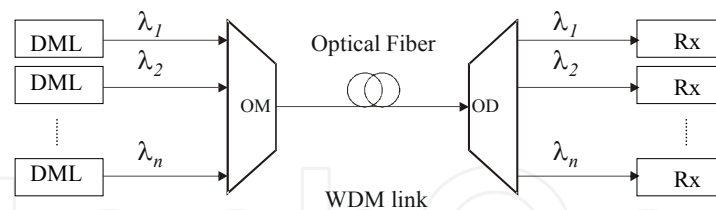

Fig. 1. Proposed optical transmission system.

The transmitter block diagram implemented in our studies consists of a bit random generator, which determines the sequence of bits, a_k, that will be sent to an electric pulse generator, in NRZ format, which injects a modulation current, $I(t)$ into the laser diode (DML), uncooled. A block diagram of the directly modulated transmitter to be considered is illustrated in Fig. 2.
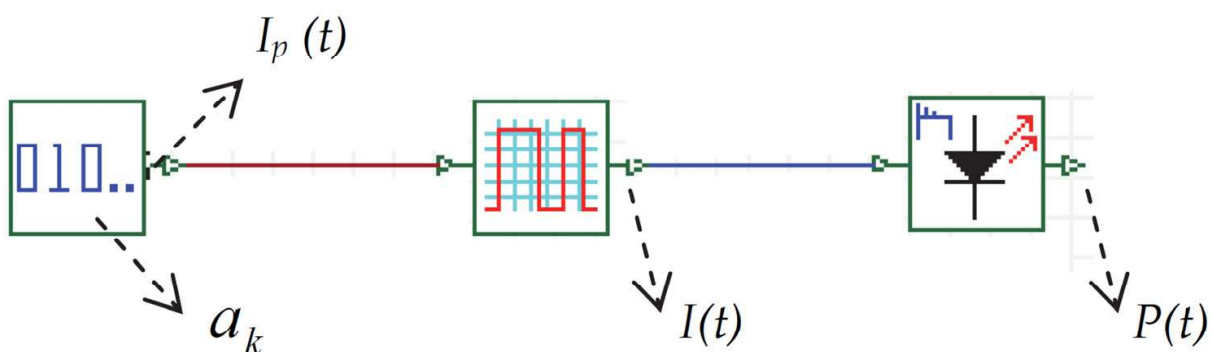

Fig. 2. Directly modulated laser scheme.

The injected laser current is given by the expression (Hinton & Stephens, 1993)

$$I(t) = I_b + \sum_{k=-\infty}^{\infty} a_k I_p(t - kT) \tag{6}$$

where I_b is the bias current, T is the period of the modulation pulse, a_k is the sequence of bits transmitted ($a_k = 1$ (0) if a binary one (zero) is transmitted during the k_{th} time), and $I_p(t)$ is the applied current pulse.

In a free-chirp source, the optical power output pulse of the laser, $P(t)$, is given by

$$P(t) = \eta_0 \cdot \frac{h\nu}{q} \cdot \sum_{k=-\infty}^{+\infty} a_k I_p(t - kT) \tag{7}$$

where η_0 is the differential quantum efficiency of the laser, $h\nu$ the photon energy at the optical frequency ν, and $I_p(t)$ the applied current pulse.

However, expression (7) is not applicable in case of directly modulated sources where the injected current that modulates the laser introduces a shift in the emission frequency (chirp frequency). As a consequence, the optical power output pulse is not a linear transformation of the applied current pulse.

3.1 Power and chirp waveform from the laser

The optical power and chirping response of the semiconductor laser to the current waveform $I(t)$ is determined by means of the large-signal rate equations, which describe the interrelationship between the photon density, carrier density, and optical phase within the laser cavity.

To calculate the optical power at the laser output depending on the value of the modulation current, we take into account the equations for the dynamics of the laser, which are given by the relationships between the density of photons $S(t)$, density of carriers $N(t)$ and the phase of the electrical field $\phi(t)$. In this way, the variation in carriers is related to the current waveform injected into the active layer $I(t)$ (Cartledge & Srinivasan, 1997; Cartledge et al. 1989; Corvini, 1987), in accordance with the following expression

$$\frac{dN(t)}{dt} = \frac{I(t)}{qV} - G[N(t) - N_t]S(t) - \frac{N(t)}{\tau_n} \tag{8}$$

and the variation of photons is given by:

$$\frac{dS(t)}{dt} = \Gamma G[N(t) - N_t]S(t) - \frac{S(t)}{\tau_p} + \frac{\beta \Gamma N(t)}{\tau_n} \quad ; \quad G = g_0 / [1 + \varepsilon S(t)] \tag{9}$$

where N_t is the carrier density at transparency, q the electron charge, V the volume of the active region, τ_n the electron lifetime, Γ the mode confinement factor in the cavity, β is the fraction of spontaneous emission coupled to the laser mode, τ_p the photon lifetime and G is the gain non-linear coefficient, ε being the compression factor of gain, g_0 the gain slope constant given by $g_0 = a_0 v_g$, where a_0 is the active layer gain coefficient and v_g the group velocity.

Thus, direct modulation of the laser current not only imprints the desired transmit data onto the emitted optical intensity, but also leads to a modulation of the carrier density within the laser cavity and in turn to a modulation of the refractive index of the active region. This in turn leads to the modulation of the frequency of the emitted light, a phenomenon that is known as laser chirp (the emission frequency must fulfil the phase condition all the time in order for the laser oscillation to occur). The chirp supposes that, even with singlemode lasers, the value of the instantaneous frequency of the emission is not the same during the optical pulse.

The frequency chirp Δv (deviation of the optical frequency at around the unmodulated frequency) is described by the coupled rate equations of the carriers and the optical field in the laser and their analytic solution yields an expression:

$$\Delta v = \frac{1}{2\pi} \frac{d\phi}{dt} \tag{10}$$

ϕ being the optical phase, whose variation with the time depends on the linewidth enhancement factor or the Henry factor α (Henry, 1982):

$$\frac{d\phi}{dt} = \frac{1}{2}\alpha \left[\Gamma v_g a_0 (N(t) - N_t) - \frac{1}{\tau_p} \right] \tag{11}$$

The linewidth enhancement factor α describes the relationship between how the real and imaginary refractive indices are affected by the carrier density. Factor α provides a measure of the coupling strength between the intensity and frequency modulation (FM) of the laser diode. It is defined as (Coldren & Corzine, 1995)

$$\alpha \equiv -\frac{dn/dN}{dg/dN} \qquad (12)$$

Here, n is the real part of refractive index of the laser cavity. dg/dN is also known as the differential gain. From (10) and (11), the amount of frequency modulation is proportional to the linewidth enhancement factor which is typically between 4-10 but can be as low as 1 in some active materials.

The output power $P(t)$ is related to the photon density $S(t)$ through the expression

$$P(t) = \frac{V\eta h\nu}{2\Gamma \tau_p} \cdot S(t) \qquad (13)$$

where h is the Planck constant and η is the differential quantum efficiency.

From the above equations the expression that relates the chirp with the laser output power can be obtained

$$\Delta \nu = \frac{\alpha}{4\pi}\left[\frac{1}{P(t)} \cdot \frac{dP(t)}{dt} + \kappa P(t) \right] \qquad (14)$$

κ being the adiabatic chirp coefficient, which is directly related to the non-linear gain compression factor

$$\kappa = \frac{2\Gamma}{V\eta h\nu} \cdot \varepsilon \qquad (15)$$

The first term in (14), is a structure-independent transient chirp and it produces variations in the pulse temporal width, while the second term is a structure-dependent adiabatic chirp, that produces a different frequency variation between the 1 and 0 bits (if the frequency of "1" is greater than the "0", it means a blue shift) causing a shift in time between the levels corresponding to "1"and "0" when the pulses go through a dispersive media, such as the optical fiber (Koch, 1988; Hakki, 1992).

DMLs can be classified according to their chirp behavior; Transient-chirp dominated DML when the first term of (14) is predominant and adiabatic-chirp dominated DML when the first term of (14) can be ignored compared to the second term of (14) (Hinton & Stephens, 1993). In following sections, we have called a DMLs with a strongly transient chirp dominated behavior DML-T and DML-A when its behavior is strongly adiabatic chirp dominated.

Fig. 3 shows the simulated power (a and c) and chirp (b and d) waveforms for two different DMLs. In this simulation, the modulating current $I(t)$ was made up of 2.5-Gb/s Gaussian current pulses.

In the case of an adiabatic chirp dominated laser (DML-A), 1 and 0 bits have a different frequency proportional to their optical power. The "0" frequency is smaller than the "1"'

frequency [see Fig. 3 (b)]. While, in the case of an adiabatic chirp dominated laser (DML-T), the power waveform shows a large power overshoot on the 1's [see Fig. 3 (c)], and the chirp has a significant value during transition states. Both behaviors are consistent with (14)
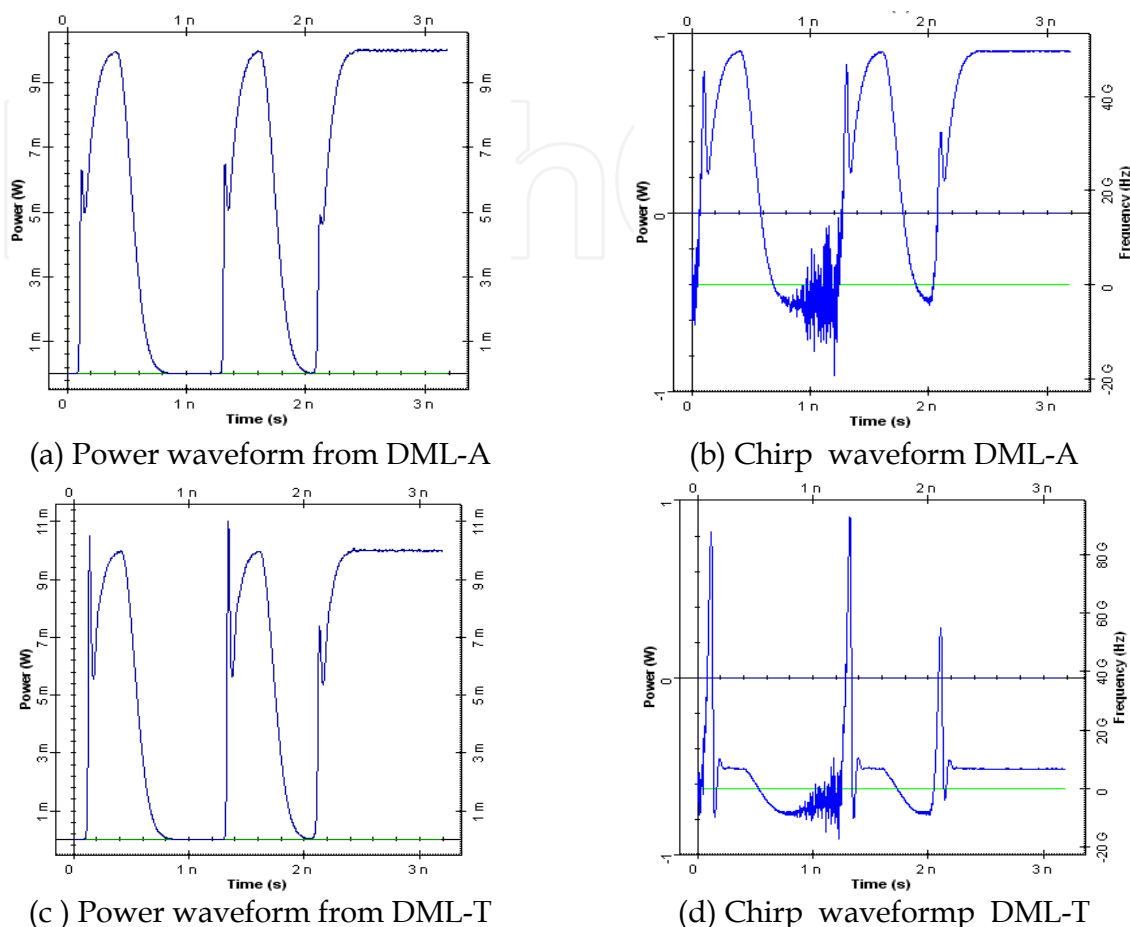

(a) Power waveform from DML-A

(b) Chirp waveform DML-A

(c) Power waveform from DML-T

(d) Chirp waveformp DML-T

Fig. 3. Simulated power (left-hand column) and chirp (right-hand column) waveforms for 2.5-Gb/s DML-A (a and b) and DML-T (c and d).

It is important to highlight that through (6-14) the frequency chirp for large-signal modulation can be determined directly from the shape of the modulated signal (e.g, square-wave, sine-wave, Gaussian, etc.). This simple expression is useful when discussing chirping phenomena because it clearly shows the interdependence of intensity and frequency modulation. In particular, the relative phases of frequency and intensity excursions are clearly displayed by (14), and these are of utmost importance in understanding the behavior of chirped signal transmission in dispersive media.

4. Transmission characteristics

When an optical pulse is transmitted through a dispersive media, such as an optical fiber, the intensity and shape of the optical signal at the output of the optical fiber, due to the waveform $I(t)$, are related with the dispersive characteristics of the optical fiber. This occurs because the spectral components that constitute the pulse are attenuated and/or phase shifted by different amounts. The effect of dispersion is more dramatic for ultrashort pulses since they have greater spectral widths.

The basic propagation equation that governs pulse evolution inside a single-mode fiber, considering expanding β to the third order of (1), is given by (Agrawal, 2010)

$$\frac{\partial A}{\partial z} + \beta_1 \frac{\partial A}{\partial t} + j\frac{\beta_2}{2}\frac{\partial^2 A}{\partial t^2} - \frac{\beta_3}{6}\frac{\partial^3 A}{\partial t^3} = 0 \qquad (16)$$

Upon propagation in a linear lossless dispersive medium, a monochromatic plane wave of frequency v traveling a distance z in the z direction undergoes a phase shift and the pulse will be broadened. Figure 4 shows the propagation of an initially unchirped Gaussian pulse through a fiber with anomalous dispersion (β_2 = GVD < 0). The pulse remains Gaussian, but its width expands and it becomes chirped with a decreasing chirp parameter (down-chirped). In this case the pulse has a decreasing instantaneous frequency.
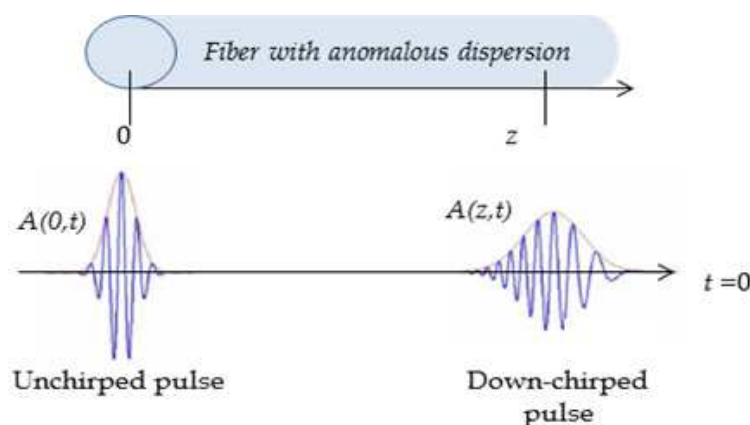

Fig. 4. Transmission of an optical pulse through a dispersive medium.

Thus, a fiber with a GVD parameter converts an unchirped Gaussian pulse of width τ_1 into a chirped Gaussian pulse of width τ_2 and chirp parameter a. Therefore, it follows that the process of pulse propagation through an optical fiber is equivalent to a combination of a time delay (second term of (16), group velocity) and a phase filter with chirp parameter b (third and fourth terms of (16) proportional to the distance z. By ignoring the third-order dispersion, the chirp parameter can be written in the form (Saleh & Teich, 2007)

$$b = 2\beta_2 z = \frac{GVD}{\pi} z \qquad (17)$$

A fiber with $\beta_2 > 0$ ($b > 0$) is said to have normal dispersion (negative dispersion coefficient, D) and it functions as an up-chirping filter which increase its instantaneous frequency. If $\beta_2 < 0$ ($b < 0$) is said to have anomalous dispersion (positive dispersion coefficient, D) and it corresponds to a down-chirping filter which decreasing its instantaneous frequency.

In normal dispersion, a blue wavelength is slower than red, so the leading edge of the pulse is red-shifted and the trailing edge is blue-shifted. The opposite occurs for anomalous dispersion.

Based on (16) and considering both the case in which the carrier wavelength is far away from the zero-dispersion wavelength (contribution of the β_3 term is negligible) and the non-linear effects in the fiber to be negligible, the fiber can be seen as a phase filter with a chirp parameter b according to (17), thus:

- For an optical fiber with normal dispersion (*b* > 0) the filter is up-chirping.
- For an optical fiber with anomalous dispersion (*b* < 0) the filter is down-chirping.

A standard single mode fiber (SSMF), optimized for the transmission in the *O-band* (~1310 nm), is a typical fiber with anomalous dispersion whose transmission characteristics are described in *Recommendation ITU-T G.652*. The negative *non-zero dispersion shifted fiber* (N-ZDSF), whose chromatic dispersion coefficient is negative in the *C-band* (and above), is an example of a normal dispersion fiber (*Recommendation ITU-T G.655).*

5. The relationship between laser chirp and dispersion

The pulse shape at a distance *z* inside the fiber is a function of different factors: the initial pulse shape, the chirp associated with this pulse from the DML and the dispersive characteristics of the optical fiber.

As already mentioned, for wavelengths far away from the zero-dispersion wavelength and considering non-linear effects in the fiber as negligible, the fiber transmission can be regarded as a phase filter with a chirp parameter *b* in accordance with (17) and with a transfer function given by (Saleh & Teich, 2007)

$$H_e(f) = \exp\left[-jb(\pi f)^2\right] \tag{18}$$

In the following sections the influence of the interplay between chirp and dispersion on a propagated pulse is examined by regarding the process of propagation as a phase filter with a transfer function governed by (19) and considering that, in accordance with (14) and (16), the optical output power from a DML is blue shifted during the pulse rise time (increasing frequency) and red shifted during the pulse fall time (decreasing frequency), that is, the pulse is a down-chirped pulse.

Firstly, we are going to consider the propagation of a chirped-Gaussian. Although the Gaussian pulse has an ideal shape that is not encountered exactly in practice, it is a useful approximation that lends itself to analytical studies. In section 5.2 a general formula is derived that can be used to evaluate the waveform of a chirped pulse of arbitrary shape.

5.1 Propagation of chirped-Gaussian pulses in an optical fiber

A general Gaussian pulse has a complex envelope *A(z,t)*

$$A(z,t) = A_0 \exp\left[-\frac{1}{2}(1 - ia_1)\frac{t^2}{T_0^2}\right] \tag{19}$$

where A_0 is the peak amplitude, T_0 represents the half-width of the pulse at the $1/e$ power point. The parameter a_1 in (19) takes into account the frequency chirp of the DML at z = 0 (ignoring the adiabatic chirp, $\kappa = 0$).

When a chirped Gaussian pulse, defined by (19), is transmitted through a phase filter, with a transfer function given by (18), the outcome is also a chirped Gaussian pulse. Thus, the shape waveform of the filtered pulse, after a distance z, is given by the equation governing the evolution of the complex amplitude of the field envelope along the fiber, *A (z, t)*

$$A(z,t) = \frac{A_0}{\sqrt{1-ja_2} \cdot \dfrac{T_1}{T_0}} \exp\left[-\frac{(1-ja_2)}{2T_1^2}t^2\right] \tag{20}$$

where

$$\frac{2T_1^2}{1-ja_2} = \frac{2T_0^2}{1-ja_1} + jb \tag{21}$$

T_1 *is* the half-width similar to T_0.

Equating the real and imaging parts of (21) leads the width T_1 and the chirp parameter a_2 associated with the pulse after a distance z

$$b_f(z) = \frac{T_1}{T_0} = \left[\left(1 + \frac{a_1 b}{2T_0^2}\right)^2 + \left(\frac{b}{2T_0^2}\right)^2\right]^{1/2} = \left[\left(1 + \frac{a_1\beta_2 z}{T_0^2}\right)^2 + \left(\frac{\beta_2 z}{T_0^2}\right)^2\right]^{1/2} \tag{22}$$

$$a_2 = a_1 + \left(1 + a_1^2\right)\frac{b}{2T_0^2} \tag{23}$$

Therefore, when a Gaussian pulse with an initial chirp a_1, travels a distance z in a dispersive media, the outcome is also a chirped Gaussian pulse with altered parameters. The chirp parameter will acquire a new value given by a_2 and the pulse will be broadened (or compressed) by a factor b_f.

In summary, as expected, the shape of the signal at the output of the optical fiber is affected by the sign of both β_2 (fiber parameter) and a (transmitter parameter). Compression can occur if an up-chirped pulse travels through a down-chirping (anomalous) medium, or if a down-chirped pulse travels through an up-chirping (normal) medium.

Taking into account the relationship between β_2 and D given by (5), Fig. 5 shows the pulse broadening factor b_f as a function of the accumulated dispersion, DL for an initial chirped Gaussian pulse from a DML with $T_0 = 30$ ps (equivalent to the bit period for a 10-Gb/s signal), dynamic chirp only, and a wavelength $\lambda = 1550$ nm and different chirp values (0, ±2 y ±4). In this case, the chirp parameter a_1 in (23) is the linewidth enhancement factor α given by (12). In order to be congruent with the notation used here, a_1 is taken as -α.

When comparing the result for the chirped pulses with $\alpha = 2$ or 4 (DML) with the result for the unchirped pulse ($\alpha = 0$), it is observed that for $D > 0$ (SMF fiber), the presence of chirp leads to significantly increased dispersion-induced pulse broadening, which increases in line with the increased chirp. However, for up to a certain amount of negative dispersion (N-NZDSF fiber), the chirp is actually beneficial and leads to pulse compression so that one can enhance the transmission system behavior.

From Fig. 5, it is observed that there is an optimum value for the accumulated dispersion that leads to minimum-width pulse. To determine the value b_{min} at which the pulse has its minimum width $T_1^{\min}$, the derivative of T_1 in (22) with respect to b is equated to zero. The result is (Saleh & Teich, 2007).
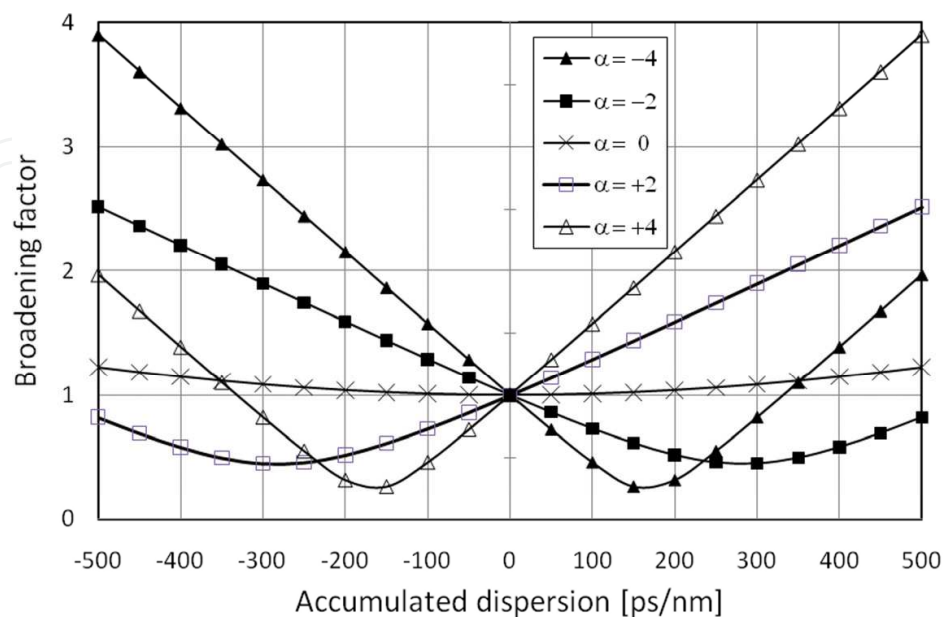
Fig. 5. Calculated pulse broadening factor b_f as a function of the accumulated dispersion: DL.

$$T_1^{\min} = \frac{T_0}{\sqrt{1 + a_1^2}}$$

$$b_{\min} = -a_1 \left(T_1^{\min}\right)^2 = -2\frac{a_1}{1 + a_1^2}T_0^2 \tag{24}$$

From (245) we can calculate the fiber length at which the width $T_1^{\min}$ is reached

$$z_{\min} = -\frac{a_1}{\beta_2\left(1 + a_1^2\right)}T_0^2 \tag{25}$$

Based on (25) z_{min} only exists for $a_1\beta_2 < 0$.

As an example, Fig. 6 (a) shows the simulated waveform of a positive chirped Gaussian pulse together with the chirp pulse when it is propagated through a negative dispersion fiber for three fiber lengths. Fig. 6 (b) represents the chirped Gaussian pulse and the phase throughout the pulse ($L_1 < L_2 < L_3$). The minimum width is reached at a length L_2 in accordance with (24). It is important to highlight that the minimum width $T_1^{\min}$ is obtained when the chirp value is zero (total compensation between DML-chirp and dispersion) and the accumulated phase is constant. Based on this, we will demonstrate the enhancement performance of an optical system by researching a modulation current waveform so that a constant accumulated phase, along the link, is achieved.

(a) Gaussian pulse and chirp.
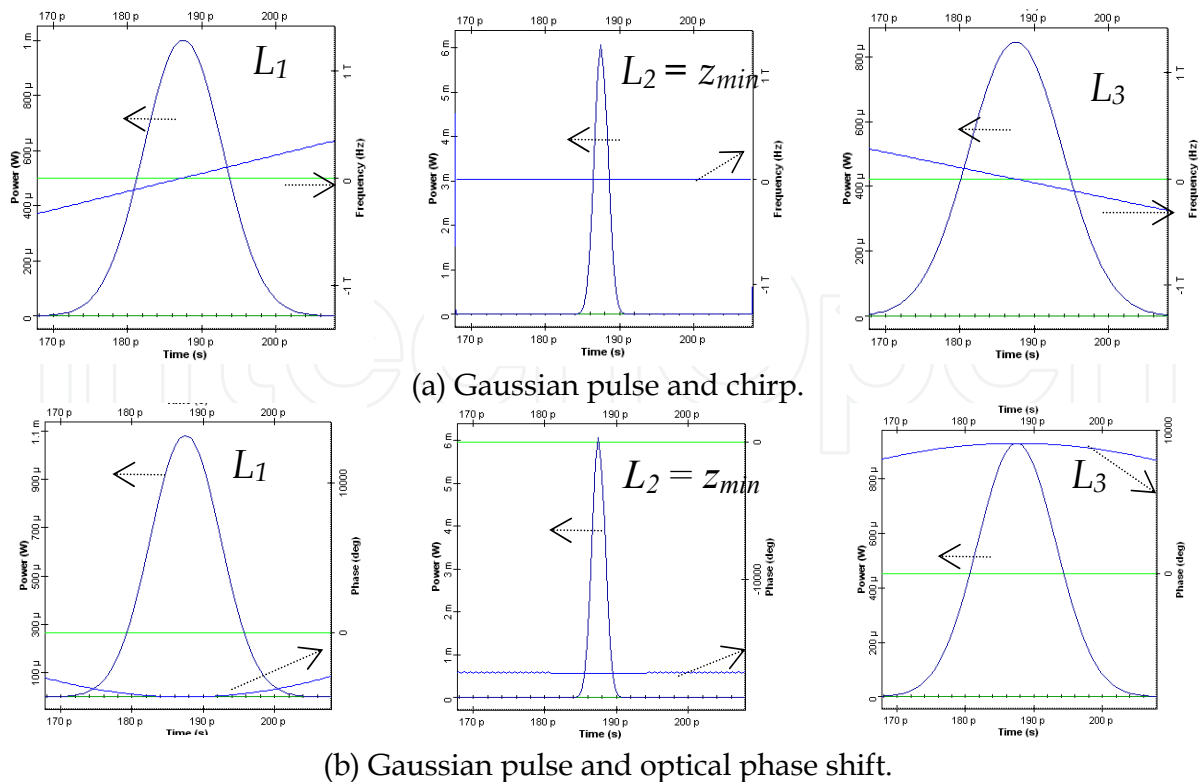

(b) Gaussian pulse and optical phase shift.

Fig. 6. Simulated waveform of a positive chirped Gaussian pulse and chirp (a) when the pulse is propagated through a negative dispersion fiber for three fiber lengths. Chirped Gaussian pulse and phase throughout the pulse (b).

5.2 Chirped pulses of arbitrary shape

Equation (20) only describes the propagation of a Gaussian pulse and includes dispersive effects only up to the second order (β_2). In practice, the pulses cannot be considered Gaussian, mainly for two reasons; as is demonstrated in Section 3.1. The pulse waveform of a DML exhibits an overshoot and ringing in its output power whilst, on the other hand, if a higher-order dispersion governed by β3 is included in (20), the pulse no longer remains Gaussian on propagation because it develops a tail with an oscillatory structure (Agrawal, 2010).

For pulses of an arbitrary shape, a measurement of the pulse width is provided by the *root mean square* (RMS) width of the pulse defined as:

$$\sigma_p = \left(\left\langle t^2 \right\rangle - \left\langle t \right\rangle^2 \right)^{1/2} \quad ; \quad \left\langle t^m \right\rangle = \frac{\int\limits_{-\infty}^{\infty} t^m \left| A(z,t) \right|^2 dt}{\int\limits_{-\infty}^{\infty} \left| A(z,t) \right|^2 dt} \tag{26}$$

Then, the broadening factor is given by

$$\frac{\sigma^2}{\sigma_0^2} = \left(1 + \frac{a\beta_2 z}{2\sigma_0^2} \right)^2 + \left(\frac{\beta_2 z}{2\sigma_0^2} \right)^2 + \left(\frac{\beta_3 z \left(1 + a^2 \right)}{4\sqrt{2}\sigma_0^3} \right)^2 \tag{27}$$

where σ_0 is the input pulse ($\sigma_0 = T_0/\sqrt{2}$). The last term in (27) is the third-order dispersion contribution to the pulse broadening.

If the complex envelope of the optical field at the laser output is given by (Agrawal, 2010)

$$A(0,t) = \sqrt{P(t)} \exp[j\phi(t)] \tag{28}$$

where $P(t)$ is the laser output power and $\phi(t)$ is obtained by the integration of (11).

The output signal complex envelope is obtained by the convolution of the input envelope (28) with the fiber response $h_e(z,t)$ [Fourier transform of (18)]. Thus, the output power at a z point is calculated as

$$P_z(t) = \left| A(z,t) * h_e(z,t) \right|^2 \tag{29}$$

Starting from (29) the shape of a chirped pulse can be determined when it is propagated through fibers with both positive and negative dispersion values.

In general, (29) cannot be easy to solve in an analytic form. In this case, computer simulations are useful to predict the exact influence of the interplay of chirp and dispersion on transmission performance.

The purpose of the following section is to present simulation results pertaining to the transmission of chirped optical signals in a dispersive fiber. In the following, it will be shown that transient-chirp dominated lasers perform better over negative and positive dispersion fibers than adiabatic-chirp dominated lasers. It will be also shown that the transient component of the chirp improves the transmission performance significantly over positive dispersion fibers if the modulation current waveform is chosen appropriately.

6. System model

Good modulation performance at high bit-rates, to avoid excessive back-to-back penalties, is one of the main requirements for CWDM transmitters. Since the *a* parameter (including the α factor and κ coefficient) is tunable by means of the modulating current $I(t)$. The optimum operating conditions in terms of the chirp/dispersion interactions can be set for fibers having different amounts and signs of dispersion. It is the aim of this section to discuss and compare how the shape of the modulated signal (e.g. square-wave, sine-wave, Gaussian, etc.) can improve the system performance when using both positive and negative dispersion fibers.

As already mentioned, numerical simulation will be required to model the exact influence of the interplay between chirp and dispersion on transmission performance. The decision on the choice of the transmission fiber characteristics (i.e., absolute dispersion value and its sign) and the DML characteristics (adiabatic or transient) for Metro applications should first be determined through simulations. The parameters of the components involved in the simulation should be sufficiently accurate and representative of the majority of commercially available components, so that useful conclusions on the design and performance of the real system can be obtained. Our simulations are based on commercial software for optical transmission systems and the component parameters used in it have been extracted from the datasheet of trademarks.

Fig. 1 shows the basic CWDM link implemented in our simulations. In this work we are specifically interested in how an optical system is impacted by the pulse shape of

modulation current. But our final purpose is to optimize a CWDM system for use in a metropolitan area optical network. Due to the chirping frequency, when a directly modulated laser is used, the system performance is very sensitive to the presence of spectrally selective components (such as multiplexers, demultiplexers and filters) in the link. As has already been shown analytically in previous sections, the shape of the pulse and its accumulated phase change as a result of their transmission through these components. For this reason, we have simulated the WDM link as shown in Fig. 1, including the optical multiplexer (OM) and demultiplexer (OD) components. Nevertheless, for the sake of clarity in analyzing the results, only the data related to one channel (i.e. the channel allocated at 1551 nm) are presented here. A summary of the most representative parameters used in our simulation is detailed below.

6.1 Optical fibers

As already mentioned, the chromatic dispersion coefficient, both in absolute terms and in sign, is one of the most influential fiber parameters in transmission performance when a DML is used as a transmitter. For this reason, in this work, we have simulated two fibers with opposite signs in their dispersion coefficient; the already laid and widely deployed, single-mode ITU-T G.652 fiber (SMF) and the ITUT-T G.655 fiber (N-NZDSF). It is well known that the SMF fiber dispersion coefficient is positive in the telecommunication band spectrum, from the *O-band* to the *L-band*, and the dispersion coefficient sign of the N-NZDSF fiber is negative around C-band.

In this work, spectral attenuation coefficient, dispersion slope, effective area and the non-linear index of refraction are compliant with SMF-28e and MetroCor Corning® commercial fibers. These fibers are in compliance with ITU-T G.652D and ITUT-T G.655, respectively.

Table I summarizes the values of the extracted parameters for the two fibers at 1551 nm wavelength.

	SMF	N-NZDSF
Attenuation Coefficient (dB/km)	0.20	0.20
Dispersion [ps/(nm·km)]	18	-5.6
Zero dispersion wavelength (nm)	1313	1605
Effective Group Index of Refraction	1.4682	1.469

Table I. Parameters for the two fibers at 1551 nm wavelength.

6.2 Transmitter

Distortion in the dispersion-induced waveform is the greatest hindrance that the designer of metro area networks has to contemplate. This distortion in the dispersion-induced waveform can have serious negative effects on the signal transmission, even at very short distances depending on the optical transmitter chosen and the characteristics of its frequency chirp.

The transmitter block diagram implemented in our simulations is shown in Fig. 2. The pulse string was encrypted with a $2^{15}-1$ pseudo-random bit sequence, OC-48 system, at 2.5 -Gb/s.

For our purpose, the leading and tailing edges of the applied current pulse $I_p(t)$ have been matched to different forms; exponential, sine and Gaussian (see Fig. 7) .

Exponential: Gaussian: Sine:

$$I_p(t) = \begin{cases} 1 - e^{-(t/c_r)} \to 0 \leq t \leq t_1 \\ 1 \to t_1 \leq t \leq t_2 \\ e^{-(t/c_f)} \to t_2 \leq T_b \end{cases} \qquad I_p(t) = \begin{cases} e^{-(t/c_r)^2} -1 \to 0 \leq t \leq t_1 \\ 1 \to t_1 \leq t \leq t_2 \\ e^{-(t/c_f)^2} \to t_2 \leq T_b \end{cases} \qquad I_p(t) = \begin{cases} sin(\pi t/c_r) \to 0 \leq t \leq t_1 \\ 1 \to t_1 \leq t \leq t_2 \\ sin(\pi t/c_f) \to t_2 \leq T_b \end{cases} \quad (30)$$

where, c_r and c_f are the rise and fall time coefficients, respectively. t_1 and t_2, together with c_r and c_f, are numerically determined to generate pulses with the exact values of the rise time and fall time parameters, and T_b is the bit period. In all simulated cases, fall and rise time are fixed at the half bit period.

Fig. 7. Exponential, Gaussian and sine pulse shape for the laser modulation current.

To simulate the DMLs, the Laser Rate Equations introduced in (Cartledge & Srinivasan, 1997; Tomkos et al., 2000) has been used as model.

	DML-A	DML-T
Factor α	2.2	5.6
Volume active layer (cm³), V	$5.8 \; 10^{-12}$	$1.1095 \; 10^{-10}$
Gain compression coefficient (cm³), ε	$5 \; 10^{-18}$	
Quantum efficiency, η	0.19	
adiabatic coefficient, κ (Hz/W)	$28.7 \; 10^{12}$	$1.5 \; 10^{12}$

Table II. Simulation parameters for directly modulated lasers DML-A and DML-T.

In the simulation, we have chosen the values of commercial lasers to generate two types of chirp behavior: DML-A with a dominant adiabatic chirp and DML-T with a dominant transient chirp. For this, we work with two typical values for the Henry coefficient, (α) (Yu & Guido, 2004; Villafranca et al, 2008; del Rio & Horche, 2008) and the adiabatic coefficient (κ) have been determined from the parameters ε, η, and Γ, in accordance with (17). These values are detailed in Table II.

6.3 Other components
The optical receiver was modeled as a *pin* photodiode with a *Responsivity* of 1 A/W and with a thermal noise of 1.84375 *10⁻²² W/Hz, followed by a low-pass Bessel electric filter to eliminate high-frequency noise.

The WDM multiplexer and demultiplexer components are configured as optical Bessel filters (2nd order) with a bandwidth of 10 GHz. They are fixed in all simulations.

6.4 Evaluation of system performance

Four different systems have been analyzed in the computer simulations, all based on the optical link shown in Fig. 1; using a DML-A in conjunction with SMF and N-NZDSF fibers, and the same scheme by substituting the DML-A by the DML-T. The performance of the systems is evaluated and the results are compared.

The transmission system performance is often characterized by the *Bit Error Rate* (BER), which is required to be less than 10^{-15} for systems with a bit rate greater than 2.5-Gb/s. Experimental characterization of these systems is difficult since the direct measurement of the BER involves considerable time and cost at such a low BER value. Another way of estimating the BER is by calculating the Q-factor of the system, which can be modeled more easily than the BER. The BER, with the optimum setting for the decision threshold, depends on the *Q-factor* as (Alexander, 1997)

$$BER = \frac{1}{2} erfc \left(\frac{Q}{\sqrt{2}} \right) \approx \frac{1}{\sqrt{2\pi}} \frac{e^{-\frac{Q^2}{2}}}{Q}; \qquad Q = \frac{|I_1 - I_0|}{\sigma_1 + \sigma_0} \tag{31}$$

where, I_i and σ_i are average and variance values, respectively, of the 1 and 0 bits.

On the other hand, the Q-factor can be determined from *eye diagram*. The eye diagram provides a visual way of monitoring the system performance: The "*eye opening*" is affected by the dispersive effects accumulated along inside the link and a closing of the eye is an indication that the system is not performing properly. If the effect of laser chirp is small, the eye closure Δ can be approximated by (Keiser, 2010)

$$\Delta = \left(\frac{4}{3} \pi^2 - 8 \right) t_{chirp} DLB^2 \delta\lambda \left[1 + \frac{2}{3} \left(DL\delta\lambda - t_{chirp} \right) \right] \tag{32}$$

where t_{chirp} is the duration of the chirp, B is the bit rate, D the fiber chromatic dispersion, L is the fiber length and $\delta\lambda$ is the maximum wavelength excursion induced by the chirp.

From (32), one approach to minimize the chirp effect is to work at the fiber zero dispersion wavelength. However, in WDM systems each channel has its own dispersion coefficient and it is not possible to implement this solution. Another way of minimizing the chirp effects, whatever the working wavelength, has to be found.

In the following section, the performance of the simulated systems is evaluated in terms of the Q-factor.

7. Simulations and results

For the simulation of the proposed system (Fig. 1), 100 km of optical fiber was used and, as already mentioned, only the results for the channel allocated at a wavelength of 1551 nm are presented. In all simulated cases the laser was polarized with a bias current slightly below the threshold; which means that no impact on the extinction ratio is considered.

According to (14), the DML chirp characteristics are dependent on their output optical power. In our previous works (Horche & del Rio, 2008, del Rio et al., 2011), we

demonstrated the existence of an optimum optical power that leads to a maximum *Q-factor* (Q_{max}). This is why the study includes an analysis of the systems at different output optical powers of the DML. In commercial uncooled DFB-DMLs the average modulated output power can reach 6 dBm or more at room temperature. In our simulations, a peak power for the "1" bit between 0.1 mW to 10 mW (average ~ 6 dBm) has been considered.

For each of these cases the system performance (*Q*-factor) has been analyzed taking into account the three different modulations current types given by (30).

7.1 Transmitter with dominant adiabatic chirp, DML-A

In a DML, the output optical power waveform is a function of the modulation current, as a result of using different currents, different optical pulse shapes are obtained. Fig. 8(a) shows the output optical power pulse shape of a DML-A when the modulation current takes exponential, Gaussian and sine forms, respectively.

The three pulses have the typical characteristic shape of the pulses generated by an adiabatic chirp-dominated laser. As can be seen in Fig. 8(a), for the current Gaussian modulation shape, the pulse leading edge is delayed in relation to the exponential and sine forms. This is the result of a higher *turn-on delay* (turn-on delay is the time required for the carrier density to build up to the threshold value before light is emitted). As seen in the following sections, this is one of the reasons why the system with a Gaussian current pulse presents the worst performance.
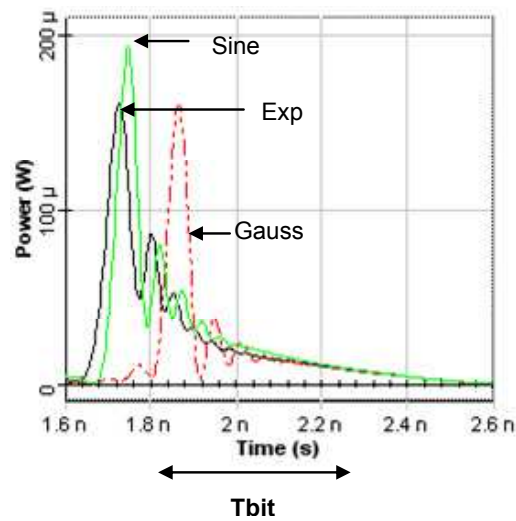
In the case of an adiabatic chirp-dominated laser, where the transient chirp has been completely "masked" by the adiabatic term, there is a shift between the frequency of the 1 and the 0 bits, the frequency of the "1" being greater than the frequency of the "0" (blue shift). Therefore, the result of the dispersion with the specific chirp characteristics is a high-intensity spike at the front of the pulses and a trailing tail-end for transmission over a positive dispersion fiber (SMF), see Fig. 8 (b). Exactly the opposite effects take place for transmission over a negative dispersion fiber (N-NZDSF), see Fig. 8 (c) [Hakki, 1992]. In the case of DML-A the main role in the transmission performance is played by the absolute value of the dispersion coefficient (rather than its sign) [Tomkos et al., 2001]. Both figures, 8(b) and 8(c), take into account the simulation of a point-to-point optical link without any selective component in wavelength, that is, only the fiber introduces changes into the chirp of the transmitted pulse.

In Fig. 9 the maximum *Q*-factor, minimum BER, of the system in Fig. 1 is shown. Variations in the DML optical power from 0.1 to 10 mW for the three types of modulation current are analyzed for an SMF, Fig. 9(a), fiber and an N-NZDSF fiber, Fig. 9 (b). The graphs show that, regardless of the type of fiber used, the system has a maximum performance for a given value of power ($P_{optimun}$) which agrees with the results obtained in previous works (Horche & del Rio, 2008; Suzuki, 1993). For low levels of channel power (P_{ch}), below the optimum power, the *Q*-factor increases with $P_{ch}(t)$, mainly because of a larger amount of power reaches the detector and the performance of the system is improved. For $P_{optimun}$ the interplay of the chirp with the dispersion leads to the best compensation between them. On the other hand, for P_{ch} higher than $P_{optimun}$, the chirp increases with the power which gives rise to a greater frequency shift between the "1" and "0" levels and linewidth broadening producing a greater optical pulse deformation.
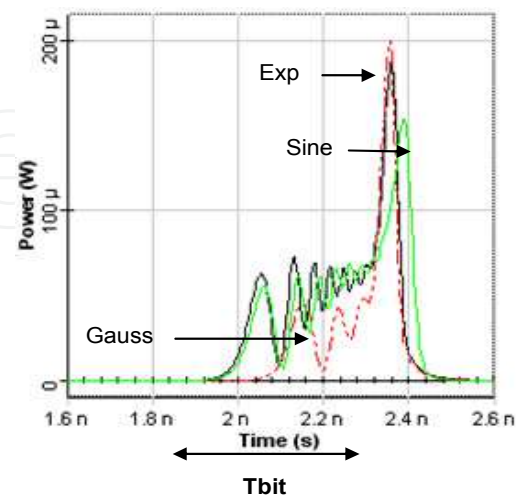
Looking at Fig. 9(a) and (b) we can see that the system has a similar behavior with the sine and exponential models and they are far from the Gaussian model. These variations are a result of the similarities/differences that exist in the shape of the pulses at the output of the laser when the different models are considered [see Fig. 8(a)].

(a) Output pulse shape of DML-A.

(b) Pulse shape after 100 km of SMF fiber

(c) Pulse shape after 100 km of N-NZDSF fiber

Fig. 8. Pulse shape for a DML-A with three types of modulation current: exponential, (thick dotted black line), Gaussian (thin dotted red line) and sine (continuous green line).
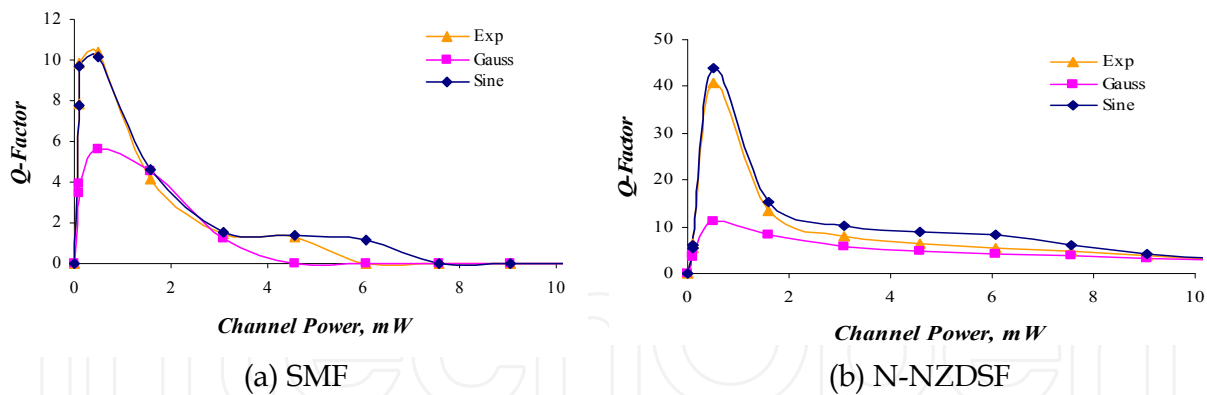
(a) SMF   (b) N-NZDSF

Fig. 9. Q-factor as a function of the DML-A output power on fibers with (a) a positive dispersion coefficient and (b) a negative dispersion coefficient.

Comparing the results from the SMF and N-NZDSF, Fig. 9(a) and (b) respectively, the N-NZDSF fiber outperforms the SMF fiber in all three cases of sine, exponential and Gaussian because of the reduced absolute dispersion value.

(a) SMF   (b) N-DSF

Fig. 10. Eye diagram for a DML-A laser with an optical output of 1 mW after 100 km of SMF (a) and N-NZDSF (b). A sine pulse is considered as the modulation current.

In Fig. 10, the eye diagrams are shown for the case of an adiabatic chirp dominated transmitter after transmission over 100 km of SMF (a) and N-NZDSF (b), respectively. In both case P_{ch} was 1 mW. The different dispersion sign will only affect the asymmetry of the eye diagram as is obvious from the results of Fig. 10.

From the simulations carried out with a DML-A transmitter, it can be concluded that with this type of laser the major factor is the absolute value of the fiber dispersion, and the waveform of the current modulation is not significant

7.2 Transmitter with a dominant transient chirp (DML-T)

Transient chirp-dominated laser diodes exhibit significantly more overshoot and ringing in output power and frequency deviations (see the power and chirp waveforms in Fig. 11). In case of a DML-T, the leading edge of the pulse is blue shifted relative to the main portion of the pulse, while the tailing edge is red shifted. The blue-shift chirped portion advances relative to the main portion of the pulses in the case of positive dispersion fibers. This effect produces a pulse spreading and consequently, an inter-symbol interference can occur.

(a)   (b)
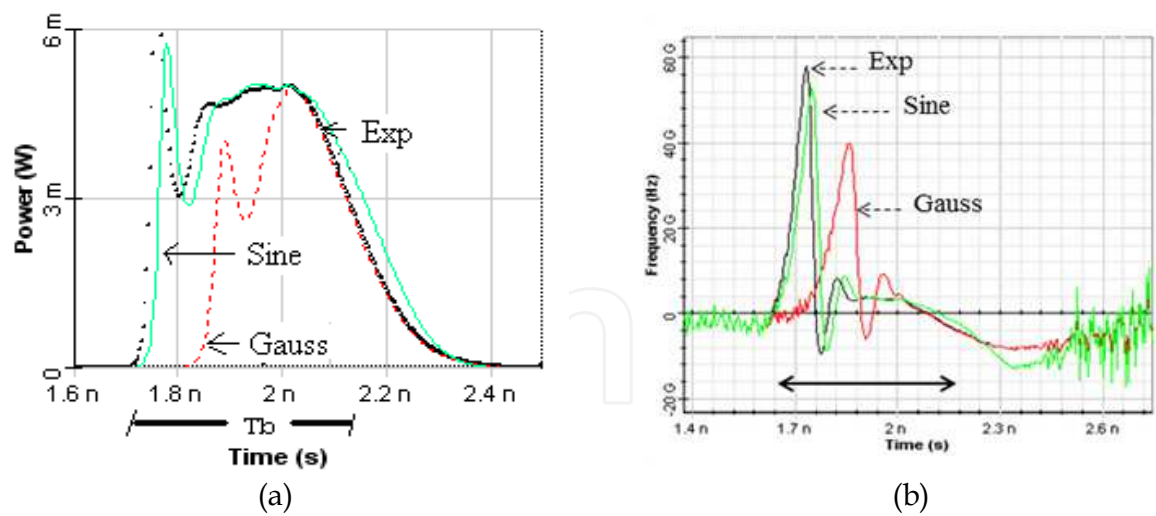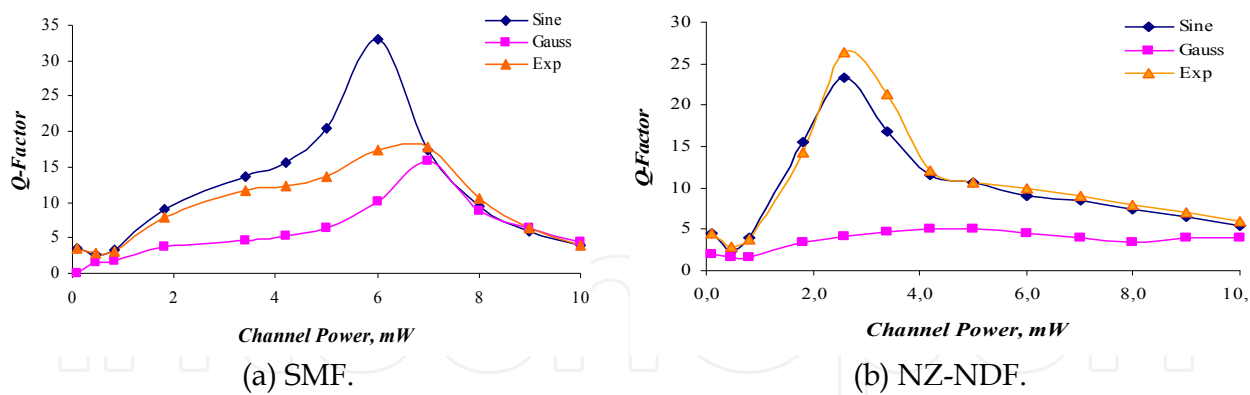
Fig. 11. Power (a) and chirp (b) waveforms for a DML-T transmitter for three different types of current modulation: exponential, Gaussian and sine.

Fig. 12 shows the *Q*-factor as a function of power for the three models studied. Fig. 12(a) corresponds to the propagation over an SMF fiber and Fig. 12 (b) is dealing with N-NZDSF. Clearly, from the results summarized in Fig. 12 some conclusions can be extracted:

- Again, the minimum quality standard is achieved for the Gaussian model
- In both SMF and N-NZDSF the existence of an optimum optical power for a maximum *Q*-factor is demonstrated. However, with the DML-T transmitter, the dispersion characteristics of the fiber used in the link determine the modulation current pulse shape for which the transmission performance is improved.

(a) SMF.   (b) NZ-NDF.

Fig. 12. Q-factor as a function of the DML-T output power on fiber with (a) a positive dispersion coefficient and (b) a negative dispersion coefficient.

Therefore, by using a negative dispersion fiber (Fig. 12(b)), the exponential current waveform is the best choice together with an output power of 2.6 mW. In this case, the reduction in quality that the sine and Gaussian pulse models have with respect to the exponential is approximately 11% and 84%, respectively.

When using an SMF fiber with a positive dispersion coefficient (see Fig. 12(a)), the modulation current with a sine shape has a better performance, particularly where the power of the laser is about 6 mW.

This improvement in performance observed with sine modulation current, can be understood in terms of the interaction that is produced between the DML-T chirp and pulse shape with the fiber dispersion; as is shown later, the accumulated phase in the received optical bit patterns is practically constant all of the time. When the chirped pulse travels along a fiber, it interacts with the fiber dispersion characteristics, causing a phase shift in the pulse, which is a function of the sign and the absolute value of the dispersion coefficient.

Fig. 13 shows the eye diagram after 100 km of SMF (a) and N-NZDSF (b) using a DML-T transmitter and when the modulation current has a sine shape. The eye corresponding to a transmission over an N-NZDSF fiber is more distorted than that corresponding to transmission over an SMF fiber. This is surprising because of the larger absolute value of the dispersion of SMF fiber compared with N-NZDSF fiber.

(a) SMF   (b) N-NZDSF

Fig. 13. Eye diagram for a DML-T laser with an optical output of 6 mW after 100 km of fiber. A sine pulse is considered as modulation current.

Through previous simulations, it has been demonstrated that directly modulated systems using SMF fibers can reach a similar (or better) Q-factor than those using N-NZDSF fibers, through the use of a correct modulation current. It means that through a suitable choice of emitted optical power in the DML together with the shape of the modulation current, the tolerance of the system at chirp can be optimized and its performance improved. This is an important conclusion since the SMF fiber is currently the most commonly installed, even when operating at 1550 nm.

8. Study of accumulated phase

All the features of the received waveforms analyzed in the previous section can be easily explained by considering the interaction of the laser chirp and pulse shape with the fiber dispersion. Then, the different Q-factors obtained with the sine, exponential and Gaussian models, when a DML-T is used together with an SMF fiber, can be justified simply by studying the accumulated phase in the bit sequence.

In the analysis of the accumulated phase, we must be very careful with the choice of the bit sequence length as the accumulated phase at reception depends on the number of transitions between the 0's and 1's in the bit pattern.

As discussed in section 3.1, the DML chirp depends on the emitted average power. Thus sending a short sequence of alternating 1 and 0 bits, the chirp fluctuates between a maximum value (when sending a "1") and a minimum (when sending a "0") and the

accumulated phase will take a constant average value. Fig. 14(a) shows the accumulated phase for a bit sequence of 8 bits (01010101). However, if the bit sequence has several identical symbols, the results can be very different. For example, Fig. 14 (b) and (c) show the accumulated phase for the "11110000" and "00001111" sequences, respectively.
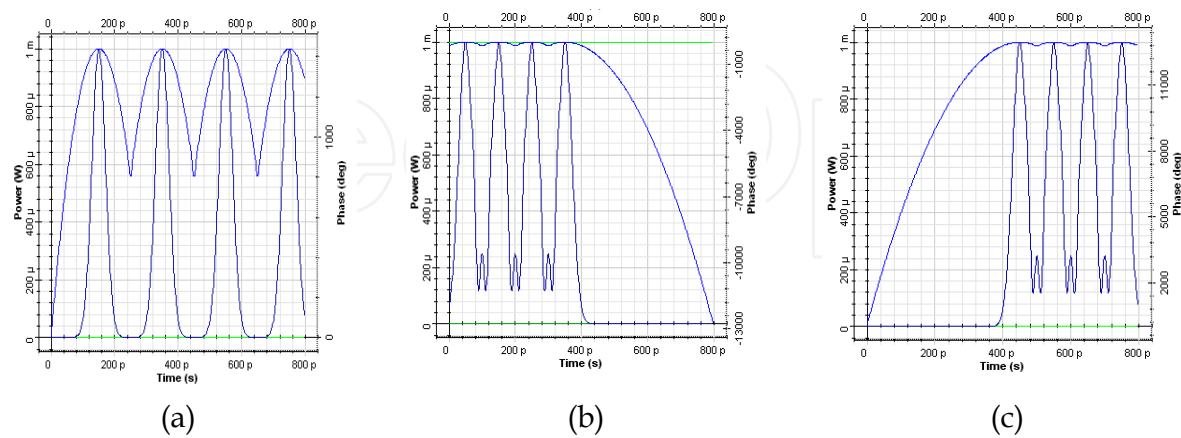

(a)   (b)   (c)

Fig. 14 The accumulated phase for a bit sequence of 8 bits (a) 01010101 (b) 1111000 and (c) 00001111.

Therefore, to obtain a result independent of the number of symbol transitions, we have to choose a large enough length sequence. On the other hand, this has the disadvantage of requiring excessively long processing times. In our simulation, we used a sequence of 512 bits, which maintains a good balance between accuracy of results and the calculation time. Fig. 15 represents the accumulated phase variation over a sequence of 512 bits, for different DML-T output power for the sine model after 100 km of SMF fiber. As can be seen, there is a single value of power (6 mW) that produces a constant phase variation over time that would be the best choice for the transmission. For this power value the phase variation is constant in time with the accumulated chirp being practically zero.
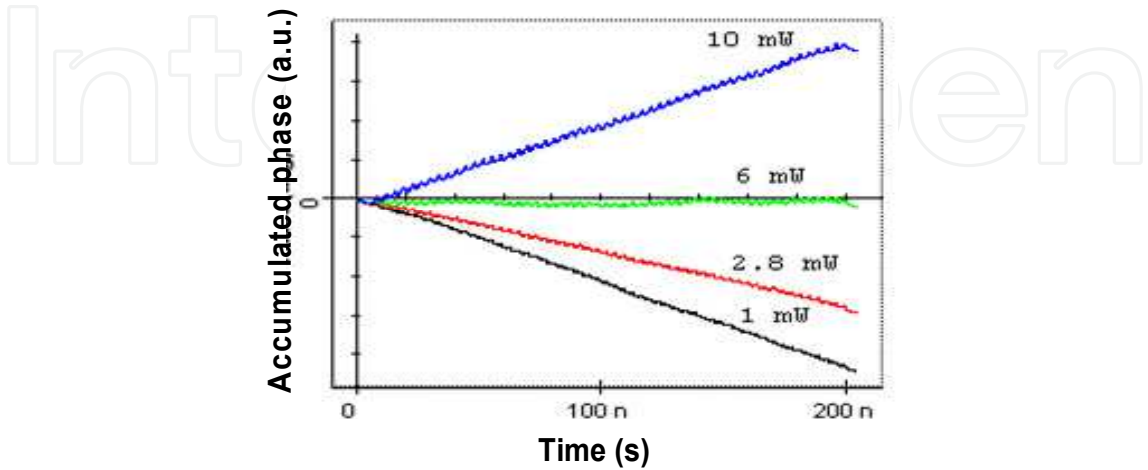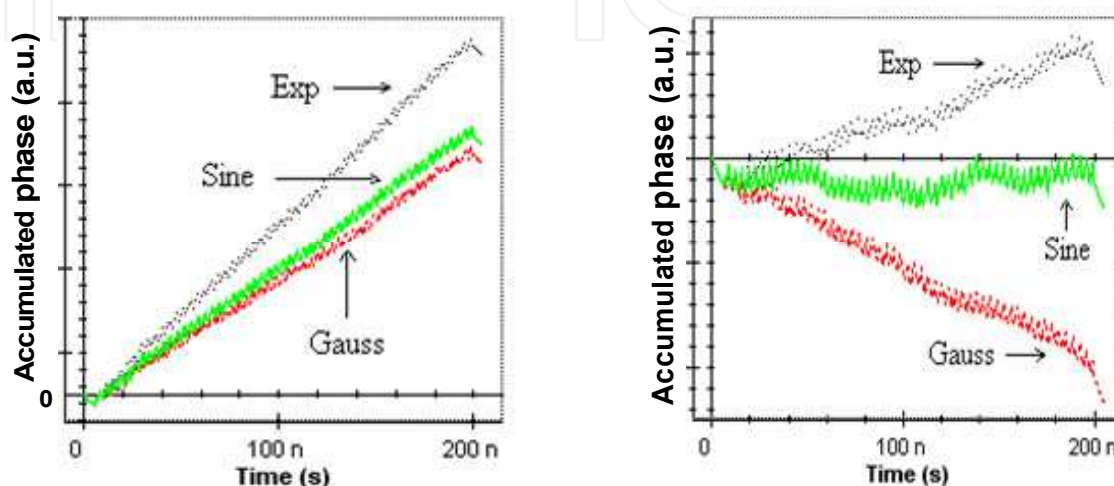

Fig. 15. Phase shifted (chirp) produced in a 512 bit sequence, for the sine model after 100 km of SMF fiber.

The accumulated phase is now represented for a sequence of 512 bits at the output of the DML-T laser with 6mW [Fig. 16(a)] and before the bit stream reaches the receiver [Fig. 16(b)], for the exponential, sine and Gaussian models. It can be seen that the bit stream goes through different accumulated phase variations when going along the SMF fiber and the filter components in the link (multiplexers, demultiplexers). The accumulated phase due to the sine pulse shape is practically constant, unlike that produced for exponential and Gaussian pulses.

(a) At the output of the DML-T laser   (b) At the output of the demultiplexer.

Fig. 16. Accumulated phase shifted (chirp) for a DML-T transmitter with 6 mW of optical power, 512-bit sequence, both before and after 100 km of SMF fiber.

The high dispersion tolerance is mainly because of the phase-correlative modulation between the adjacent bits via a precise control of the frequency chirp in the DML modulation. Therefore, based on (1-8), we can design the parameters of the DMLs (including the drive current (DC) bias) to offer a suitable chirp response for the generation of the phase correlation.

9. Analysis of transmission performance through different SMF and N-NZDSF fiber lengths

In order to get a general idea of the behavior of the systems detailed in Fig. 1 with the link length, a set of simulations was carried out by varying the fiber length, L. As in the former cases, only the results for a channel centered at 1551 nm are shown. The simulated transmitter was a DML-T similar to that used in the former sections. The output power is P_{ch}= 6 mW in case of a SMF fiber [see Fig. 12 (a)] and P_{ch}= 2.6 mW when a NZ-NDF fiber is used [see Fig. 12 (b)]. These power values have been selected to obtain the Q_{max}.

Fig. 17 represents the Q-factor versus fiber length when an SMF fiber (a) and a NZ-NDF fiber (b) are used for sine, Gaussian and exponential modulation current waveforms, respectively. As expected, the Q_{max} is reached for a fiber length of 100 km and a sine modulation current in the case of an SMF fiber. This is the length at which the interaction between the accumulated dispersion in the fiber and the chirp generated in the DML is

optimal. Nevertheless, for other fiber lengths, another choice can provide a better performance.

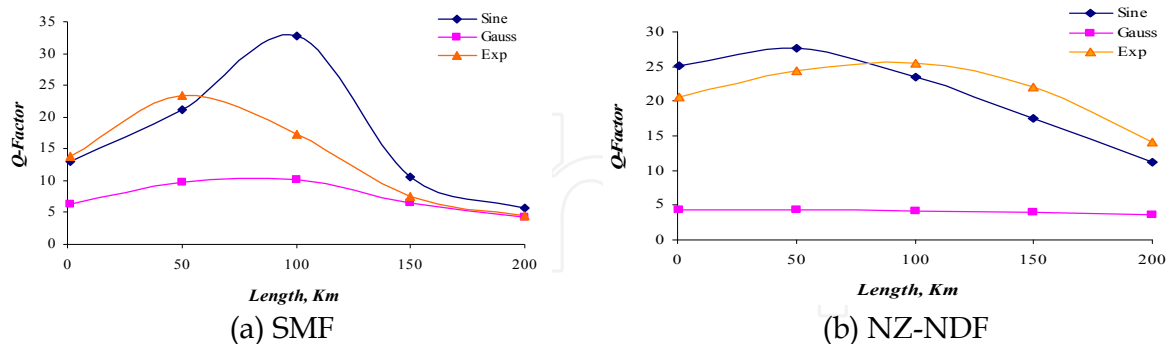(a) SMF   (b) NZ-NDF

Fig. 17. Q-factor as a function of the link distance through fibers with (a) positive dispersion coefficient and (b) negative dispersion coefficient (Pch = 6 mW).

In the case of an N- NZDSF fiber, in Fig. 17 (b), with a P_{ch}= 2.6 mW, the Q_{max} is obtained for lengths different from 100 km, i.e. for a sine modulation current, L = 50 km [not exponential as in Fig. 12 (b)]. Therefore, we can conclude that the maximum of the Q factor depends on the modulation current shape, the length of the link and the optical power at the DML output.

10. Conclusion

In this chapter we have determined the dependence of the system performance of a directly-modulated optical system as regards the shape of the optical pulse transmitted through the fiber. It has been demonstrated that, if the laser has adiabatic dominant chirp behavior (DML-A), the absolute value of the fiber dispersion coefficient will be a determinant of the system performance but the influence of the current pulse shape is not significant.

We have also demonstrated that, if the laser has transient dominant chirp behavior, it is possible to improve the performance of an already installed system by modifying the shape of the electric current that modulates the laser. As the high dispersion tolerance is mainly because of the phase-correlative modulation between the adjacent bits, then, we can design the parameters of the DMLs, including the modulating current shape, to offer a suitable chirp response for the generation of the phase correlation. For SMF fibers (positive dispersion coefficient), this shape is sinusoidal and for NZ-NDF fibers (negative dispersion coefficient), the shape is exponential, when long-haul inter-office transport systems, corresponding to link distances of about 40 - 100 km, are considered.

In summary, through the appropriate combinations of DML transmitters (adiabatic or transient) and shape current, optical fiber systems can be achieved which are optimized in terms of dispersion and cost. With this method it is possible to improve each of the WDM system channels individually, offering a low-cost solution since it only involves changes in the transmitters and avoiding the replacement of the fiber.
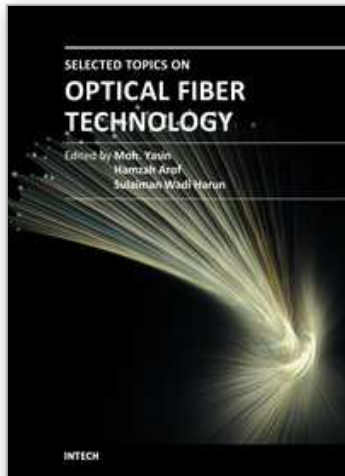
11. Acknowledgements

12. References

Agrawal, P. (2010) Fiber-Optic Communication System. *John Wiley & Sons*. ISBN 978-0-470-50511-3.

Alexander S. B. (1997). Optical Communication Receiver Design. SPIE Press/ IEE.

Cartledge, J.C. & Burley, G.S., (1989). The effects of laser chirping on lightwave system performance, *J. Lightwave Technol.*, Vol. 7, No. 3, pp. 568–573, 1989. ISSN: 0733-8724

Cartledge, J.C. & Srinivasan, R.C. (1997). Extraction of DFB Laser Rate Equation Parameters for System Simulation Purposes. *J. of Lightwave Technol.*, Vol. 15, No. 5, May 1997, pp. 852-860. ISSN: 0733-8724.

Coldren L.A., & Corzine, S.W. (1995) *Diode Lasers and Photonic Integrated Circuits*, Wiley Series in Microwave and Optical Engineering.

Corvini, P. & Koch, T. (1987). Computer Simulation of High-Bit-Rate Optical Fiber Transmission Using Single-Frequency Lasers. *J. Lightwave Technol.*, Vol. 5, No. 11, pp. 1591 - 1595. November 1987. ISSN: 0733-8724.

del Río, C. & Horche, P.R. (2008). Directly modulated laser intrinsic parameters Optimization for WDM Systems. *International Conference on Advances in Electronics and Micro-electronics*, ENICS 2008.

del Río, C., Horche, P.R., & Martín, A. (2011), Interaction of semiconductor laser chirp with fiber dispersion: Impact on WDM directly modulated system performance". *Proc. of The Fourth International Conference on Advances in Circuits, Electronics and Micro-electronics.* CENICS 2011, 22-27 August, Nize, France.

Hakki, B.W. (1992). Evaluation of transmission characteristics of chirped DFB lasers in dispersive optical fiber. *J. of Lightwave Technology*, Vol. 10, No. 7, pp. 964 – 970, Jul 1992. ISSN: 0733-8724

Henry, C. H. "Theory of the linewidth of Semiconductor Lasers". *IEEE J. of Quantum Electronics*, Vol. QE-18, pp. 259 - 264, Feb 1982. ISSN: 0018-9197.

Hinton, K.; Stephens, T.; Modeling high-speed optical transmission systems. *IEEE J. Selected Areas in Communications*, Vol. 11, Issue 3, pp. 380 - 392.

Horche, P.R. & del Río, C.. "Enhanced Performance of WDM Systems using Directly Modulated Lasers on Positive Dispersion Fibers". *Optical Fiber Technology*. Vol. 14, No. 2, pp. 102-108, April 2008.

Keiser, G., (200). *Optical Fiber Communications*. McGraw-Hill. ISBN: 978-007-108808.

Koch, T.L.; Corvini, P.J., (1988). Semiconductor laser chirping-induced dispersive distortion in high-bit-rate optical fiber communications systems. *IEEE International Conference on Communications*, ICC '88. Vol. 2, pp. 584 - 587.

Nebeling, M. (2007). CWDM Transceivers, In: *Coarse Wavelength Division Multiplexing; Technologies and Applications*. Edited by Hans-Jörg Thiele & Marcus Nebeling, pp. (57-90), CRC Press Taylor & Francis Group, ISBN-10: 0-8493-3533-7, USA.

Saleh, B.E.A., Teich, M.C., Fundamentals of Photonics. (2007). Wiley Series in Pure an Applied Optics. ISBN: 978-0-471-35832-9, USA.

Suzuki, N., (1993). Simultaneous Compensation of Laser Chirp, Kerr Effect, and Dispersion in 10 Gp/s Long-Haul Transmission Systems. *J. of Lightwave Technology*, Vol. 11, No. 9, Sep 1993. ISSN: 0733-8724

Thiele, H-J & Nebeling, M (2007) *Coarse Wavelength Division Multiplexing; Technologies and Applications*. CRC Press Taylor & Francis Group, ISBN-10: 0-8493-3533-7, USA.

Tomkos I.; Roudas, I.; Boskovic, A.; Antoniades, N.; Hesse, R. & Vodhanel, R. (2000).
        Measurements of Laser Rate Equation Parameters for Simulating the Performance
        of Directly Modulated 2.5 Gb/s Metro Area Transmission Systems and Networks.
        IEEE Lasers and Electro-Optics Society, LEOS 2000, Vol 2, pp. 692 – 693, 2000.
Tomkos, I., Chowdhury, D., Conradi, J., Culverhouse, D., Ennser, K., Giroux, C., Hallock, B.,
        Kennedy, T., Kruse, A., Kumar, S., Lascar, N., Roudas, I., Sharma, M., Vodhanel, R.
        S., & Wang, C.-C. (2001). Demonstration of Negative Dispersion Fibers for DWDM
        Metropolitan Area Networks, *IEEE J. on selected Topis in Quantum Electronics*. Vol. 7,
        No. 3, May/Jun 2001, pp. 439-460.
Villafranca, A., Lasobras, Escorihuela, J. R., Alonso, R. & Garcés, I. "Time-resolved Chirp
        Measurements using complex Spectrum analysis based on stimulated Brillouin
        Scattering" *Proceedings of the OFC*, Paper OWD4, San Diego (USA), Feb 2008.
Yu, Y., & Giuliani, G. (2004). Measurement of the Linewidth Enhancement Factor of
        Semiconductor Lasers Based on the Optical Feedback Self-Mixing Effect. *IEEE
        Photonics Technology Letters*, Vol. 16, No. 4, pp. 990 - 992. April 2004. ISSN:1041-1135
Linke, R.A. (1985). Modulation Induced Transient Chirping in Single Frequency Lasers.
        IEEE J. Quantum Electronics, Vol. QE-21, No. 6, (June 1985), pp. 593-597, ISBN
Morgado, J.A.P & Cartaxo, A.V.T. (2001). Dispersion supported transmission technique:
        comparison of performance in anomalous and normal propagation regimes. *IEE
        Proc-Optoeelctron*., Vol. 148, No. 2, (April 2001), pp. 107-116, ISBN

Selected Topics on Optical Fiber Technology

Edited by Dr Moh. Yasin

This book presents a comprehensive account of the recent advances and research in optical fiber technology. It covers a broad spectrum of topics in special areas of optical fiber technology. The book highlights the development of fiber lasers, optical fiber applications in medical, imaging, spectroscopy and measurement, new optical fibers and sensors. This is an essential reference for researchers working in optical fiber researches and for industrial users who need to be aware of current developments in fiber lasers, sensors and other optical fiber applications.

How to reference

In order to correctly reference this scholarly work, feel free to copy and paste the following:

Paloma R. Horche and Carmina del Río Campos (2012). Influence of Current Pulse Shape on Directly Modulated Systems using Positive and Negative Dispersion Fibers, Selected Topics on Optical Fiber Technology, Dr Moh. Yasin (Ed.), ISBN: 978-953-51-0091-1, InTech, Available from: http://www.intechopen.com/books/selected-topics-on-optical-fiber-technology/influence-of-current-pulse-shape-on-directly-modulated-systems-using-positive-and-negative-dispersio

INTECH
open science | open minds